in the divergent portion. This is probably because the void region gradually grows as the axial Mach number is increased. The radii of void regions near the nozzle axis were obtained by setting the denominator of Eq. (1) equal to zero.

### References


[1] Hsu, C. T., "Swirling Nozzle Flow Equations from Crocco's Relation," *AIAA Journal*, Vol. 9, No. 9, Sept. 1971, pp. 1866–1868.

[2] Hsu, C. T., "Errata: 'Swirling Nozzle Flow Equations from Crocco's Relation,'" *AIAA Journal*, Vol. 10, No. 3, March 1972, p. 368.

[3] Batson, J. L. and Sforzini, R. H., "Swirling Flow through a Nozzle," *Journal of Spacecraft and Rockets*, Vol. 7, No. 2, Feb. 1970, pp. 159–163.

[4] DeJoode, A. D., "Mach Number Distribution and Mass Flow Rate for Swirling Flow in a Choked Nozzle Throat," MS thesis, Feb. 1973, Iowa State Univ., Ames, Iowa.

[5] Lewellen, W. S., Burns, W. J., and Strickland, H. J., "Transonic Swirling Flow," *AIAA Journal*, Vol. 7, No. 7, July 1969, pp. 1290–1297.


# A Finite Element Method for the Optimal Design of Variable Thickness Sheets


M. P. ROSSOW* AND J. E. TAYLOR†

*The University of Michigan, Ann Arbor, Mich.*


### Introduction

THE nature of recent research work in the field of structures optimization is summarized (exclusive of Russian and East European activity) by Niordson and Pedersen in Ref. 1. There is evidence from their survey as well as from other sources of a trend toward greater emphasis on topics related to numerical solution. Our development of a finite element interpretation for the prediction of optimal design follows this trend. We particularly seek to establish useful means for handling two-dimensional design problems.

Several recent papers on general methods for the numerical solution of design problems relate to our work. To name a few, Haug et al.[2] developed a steepest descent procedure to calculate the optimal design of piecewise uniform structures. Also Maier et al.[3] demonstrated how the problem of designing for maximum safety relative to collapse of plane stress structures can be formulated as a linear programing problem, through the use of finite element modeling of the structure. Dafalias and Dupuis[4] made use of a discretization scheme to obtain their procedure for the solution of optimum beam design problems. Aspects of numerical solution in flutter optimization problems were discussed by Ashley and McIntosh.[5]

In some early automated design programs, a design prediction was obtained by iteration on the computer between independent design and analysis elements of a program. In contrast, our formulation amounts to having the finite element discretization incorporated into a direct design procedure. This formulation is demonstrated, and the character of the governing equations for the discretized structure is established. An example application of the formulation is provided.


Received March 26, 1973; revision received June 18, 1973. Support was received from the National Science Foundation for the research reported in this Note.

Index category: Structural Design, Optimal.



* Postdoctoral Fellow, Department of Applied Mechanics and Engineering Science.

† Associate Professor, Departments of Aerospace Engineering, and Applied Mechanics and Engineering Science. Member AIAA.


Many of the considerations associated with the problem formulation reported in this Note are treated in greater detail in the thesis of Rossow.[6]

### Problem Formulation

The optimality criterion to be used in this Note is that of maximum stiffness for a given volume of material. More precisely, if $W[t]$ represents the loss in potential of the edge loads applied to the sheet of variable thickness $t$, then an optimal design $t^*$ is defined by the relation

$$W[t^*] = \min_t W[t] \tag{1}$$

All admissible designs $t$ are required to satisfy the volume constraint

$$\int_A \int t\, dA = V_o \tag{2}$$

Here $A$ is the region in the $x$-$y$ plane occupied by the sheet, and $V_o$ is the specified volume of material.

It is convenient for subsequent developments to replace the quantity $W[t]$ by the potential energy of the sheet, $P[t]$. By Clapeyron's Theorem, we have

$$P[t] = -W[t]/2 \tag{3}$$

Thus, the maximum stiffness design problem can be restated as the problem of finding $t^*$ such that

$$P[t^*] = \max_t P[t] \tag{4}$$

where $t$ satisfies Eq. (2).

The potential energy for an elastic sheet in a state of plane stress is

$$P[t] = \frac{1}{2}\int_A \int \boldsymbol{\varepsilon}^T \mathbf{c}\boldsymbol{\varepsilon} t\, dA - \int_S (Xu + Yv)\, dS \tag{5}$$

where $u = u(x, y)$ and $v = v(x, y)$ are the displacements of the sheet in the $x$ and $y$ coordinate directions, and $t = t(x, y)$ is the sheet thickness. The elastic strain $\boldsymbol{\varepsilon}$ in Eq. (5) is given by

$$\boldsymbol{\varepsilon}^T \equiv \{\partial u/\partial x, \partial v/\partial y, \partial u/\partial y, \partial v/\partial x\} \tag{6}$$

while the elastic constants $\mathbf{c}$ represent

$$c = \frac{E}{1-\nu^2}\begin{bmatrix} 1 & \nu & 0 \\ \nu & 1 & 0 \\ 0 & 0 & (1-\nu)/2 \end{bmatrix} \tag{7}$$

Here $E$ symbolizes Young's modulus and $\nu$ the Poisson ratio. $S$ designates that portion of the boundary of $A$ where the components $X$ and $Y$ of the traction vector are specified.

Equation (4) together with Eq. (2) defines an isoperimetric problem in the calculus of variations (cf. Ref. 6). Its solution must satisfy the Euler equations with respect to $t$ of the functional comprised of the potential energy augmented by the volume constraint. The two equilibrium equations associated with $u$ and $v$ must, of course, be satisfied at the same time. (These equations are sufficient for optimality as well as necessary; see, for example, Ref. 8.)

Finding the solution of this system of three simultaneous partial differential equations will, in general, require the use of numerical methods. A particular approximating scheme based on a finite element representation of the potential energy of the sheet will now be presented.

Let the region $A$ occupied by the sheet be divided into a mesh of $n$ elements and approximate the thickness function $t$ in element $i$, $i = 1, 2, \ldots, n$, by a uniform value $\tau_i$. After also approximating the displacement field within element $i$ in the usual finite element manner, the first term on the right-hand side of Eq. (5) when evaluated over element $i$ yields

$$\frac{\tau_i}{2}\sum_{r=1}^{p}\sum_{s=1}^{p} K_{rs}{}^i \delta_r{}^i \delta_s{}^i \equiv \tau_i U_i(\delta) \tag{8}$$

Here $\delta_r{}^i$ denotes a local nodal displacement, $K_{rs}{}^i$ is a member of the element stiffness matrix, and $p$ is the number of displace-

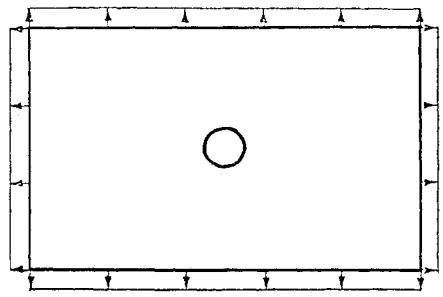

**Fig. 1a Rectangular sheet, with central opening, subjected to edge loads.**

ment degrees of freedom of the element chosen. The $U_i$ represents strain energy per unit element thickness.

Summing the contributions of all the elements, the strain energy of the discretized sheet is

$$\sum_{i=1}^{n} \tau_i U_i \equiv U(\tau, \delta) \tag{9}$$

If the local nodal displacements appearing in Eq. (9) are replaced by the corresponding global nodal displacements $\delta_j$, $j = 1, 2, \ldots, 2m$ ($m$ is the total number of nodes in the mesh), an alternative expression for the strain energy results

$$U(\tau, \delta) = \frac{1}{2} \sum_{i=1}^{2m} \sum_{j=1}^{2n} k_{ij} \delta_i \delta_j \tag{10}$$

Here the unknown element thicknesses $\tau_i$ occurring in Eq. (9) have been absorbed in the members $k_{ij}$ of the global stiffness matrix.

Introduction of the approximate displacement field in the second integral of Eq. (5) results in the quantity

$$\sum_{j=1}^{2m} F_j \delta_j \equiv W(\delta) \tag{11}$$

where the nodal forces $F_j$ are assigned a value of zero for nodes not on the boundary $S$.

The potential energy of the discretized sheet can now be written

$$P(\delta, \tau) \equiv U(\delta, \tau) - W(\delta) \tag{12}$$

The design of such a discretized sheet will be understood to mean a set of element thicknesses $\tau$: $\tau_1, \tau_2, \ldots, \tau_n$. From usual finite element theory, for given design $\tau$, the nodal displacements satisfy the equilibrium equations

$$\frac{\partial P}{\partial \delta_l} = \sum_{i=1}^{2m} k_{il} \delta_l - F_l = 0, \qquad l = 1, 2, \ldots, 2m \tag{13}$$

The global stiffness matrix is assumed modified corresponding to the boundary conditions so that Eq. (13) may be solved for a unique set of nodal displacements $\delta$. A set $\delta$ found in this way will be denoted by $\delta(\tau)$.

### The Discretized Design Problem

With the use of the notation just introduced, the problem of determining the optimal distribution of material within the discretized sheet can now be stated as follows. A design $\tau^*$ is sought such that

$$P[\tau^*, \delta(\tau^*)] = \max P[\tau, \delta(\tau)] \tag{14}$$

where admissible design $\tau$ must satisfy

$$\sum_{i=1}^{n} A_i \tau_i = V_o \tag{15}$$

$$\tau_i^L \leqq \tau_i \leqq \tau_i^U, \qquad i = 1, 2, \ldots, n \tag{16}$$

Here $A_i$ is the area of element $i$. The original design problem is extended with little effort to accommodate the constraints (16) on the design.

Conditions which an optimal discrete design must satisfy may be derived by introducing slack functions $a_i^U$ and $a_i^L$ to express constraints (16) in the form

$$\tau_i + (a_i^U)^2 = \tau_i^U, \qquad \tau_i - (a_i^L)^2 = \tau_i^L \tag{17}$$

We then form the function

$$L = P[\delta(\tau), \tau] + \lambda\left(V_o - \sum_{i=1}^{n} A_i \tau_i\right) + \sum_{i=1}^{n} \Omega_i^U [\tau_i^U - \tau_i - (a_i^U)^2] + \sum_{i=1}^{n} \Omega_i^L [\tau_i^L - \tau_i + (a_i^L)^2] \tag{18}$$

where $\lambda$, $\Omega_i^U$, and $\Omega_i^L$ are Lagrange multipliers. A necessary condition for $P[\delta(\tau^*), \tau^*]$ to be maximum is the vanishing of the first derivatives of $L$ with respect to $a_i^U$, $a_i^L$, and $\tau_i$. This leads to

$$a_i^U \Omega_i^U = 0 \quad \text{and} \quad a_i^L \Omega_i^L = 0 \tag{19}$$

and

$$\frac{\partial P}{\partial \tau_i} + \sum_{j=1}^{2m} \frac{\partial P}{\partial \delta_j} \frac{\partial \delta_j}{\partial \tau_i} - \lambda A_i - \Omega_i^U - \Omega_i^L = 0 \tag{20}$$

But $\partial P / \partial \delta_j = 0$, since equilibrium is satisfied, and furthermore

$$\partial P / \partial \tau_i = U_i$$

by Eqs. (12) and (9).

Thus, Eq. (20) becomes

$$U_i[\delta(\tau^*)] - \lambda A_i - \Omega_i^L - \Omega_i^U = 0 \tag{21}$$

An additional necessary condition follows from the Kuhn-Tucker theorem of nonlinear programing

$$\Omega_i^U \geqq 0 \quad \text{and} \quad \Omega_i^L \leqq 0 \tag{22}$$

Equation (21) represents a finite element equivalent of the uniform specific strain energy criterion for optimal design. For, suppose the thickness of element $i$ lies between the thickness constraints:

$$\tau_i^L < \tau_i < \tau_i^U$$

Then the slack variables $a_i^U$ and $a_i^L$ are not equal to zero and so Eq. (19) requires $\Omega_i^L = 0$ and $\Omega_i^U = 0$. But then Eq. (21) can be written $U_i / A_i = \lambda$. Thus, the optimal finite element structure should be designed such that the average specific strain energy in all elements (where the thickness constraints are inactive) has the same constant value $\lambda$. This result may be compared with the optimality conditions derived by Sheu and Prager in Ref. 9 for certain naturally discrete structures. It may be verified that the conditions just derived are sufficient for optimality as well as necessary.[6] We also note that the conditions correspond to those derived by Mroz in Ref. 10.

### Example

As an illustration of the preceding results, the optimal thickness distribution of the rectangular sheet shown in Fig. 1a will be calculated. The sheet is loaded on all four edges and has a circular opening of radius $r = 0.73$. A finite element mesh covering one quadrant of the sheet is shown in Fig. 1b. Quadrilateral

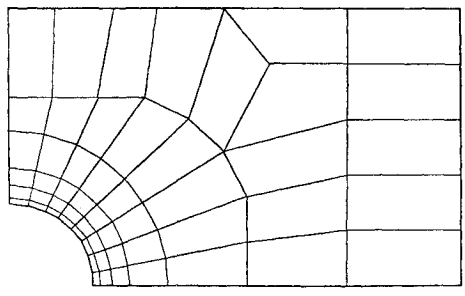

**Fig. 1b Finite element mesh for one quadrant of rectangular sheet.**

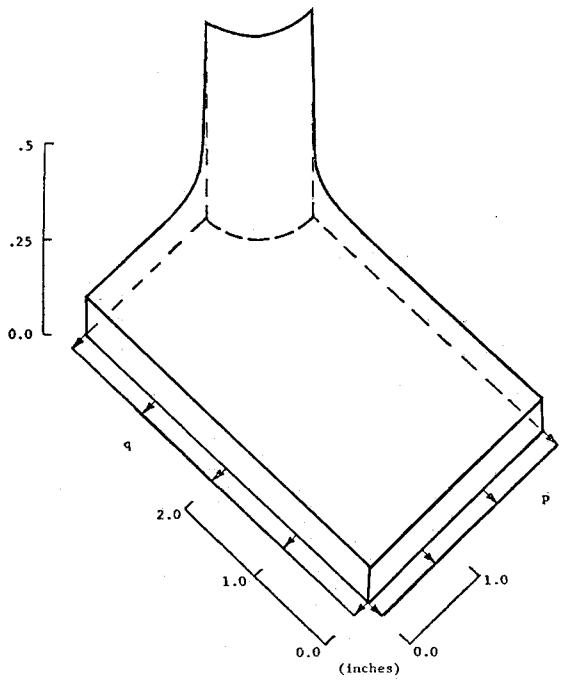


**Fig. 2 Optimal design of rectangular sheet when edge loads are equal: $p/E = 1.0$ in., $q/E = 1.0$ in.**

isoparametric elements[11] with eight degrees of freedom were used.

In order to consider the effect of varying boundary conditions at the hole (as in Ref. 12), a reinforcing ring of known elastic properties is introduced there. The cross-sectional area of the ring times the ratio of ring elastic modulus to sheet modulus is taken to equal 0.052 in.$^2$ The ring is represented in the finite element model as a series of short elastic rods connecting adjacent nodes along the boundary. The strain energy of these rods is added to the potential energy $P[\tau, \delta(\tau)]$ of Eq. (18). Since the strain energy of the rods is never negative, the positive definiteness of the global stiffness matrix is maintained, and the derivations of the previous paragraphs remain valid.

The inequality constraints in Eq. (16) are inactive for our example. In this case, Eqs. (19) and (22) are identically satisfied with $\Omega_i^U = \Omega_i^L = 0$ for all elements, and the remaining Eqs. (13, 15, and 21) can be solved by a modified version of the Newton-Raphson method. The resulting designs corresponding to different values of the edge loads are shown in Figs. 2 and 3. The smooth curves were obtained from the piecewise distribution of element thicknesses by plotting the thickness of each element at its centroid. The concentration of material indicated on the side of the hole nearest the long edge may be identified with the stress concentration that would be found in the same region of a uniform sheet.

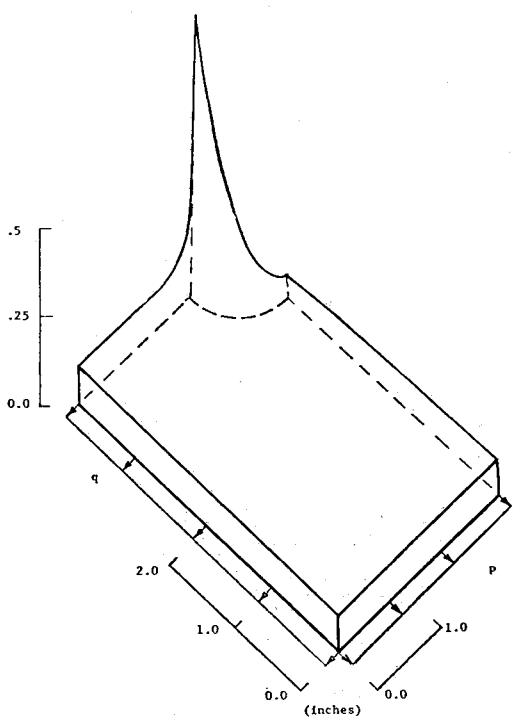


**Fig. 3 Optimal design, for unequal edge loads: $p/E = 1.0$ in., $q/E = 0.50$ in.**

## Summary

The finite element model demonstrated here is an authentic interpretation in discretized form of the original design problem. This may be judged by much the same means as are used to qualify finite element methods applied to the comparable continuum analysis problem. With the formulation of this paper the ability to obtain solutions to the design problem relates directly to methods for the numerical solution of an algebraic system, such as Eqs. (13, 15, and 21). Thus, in particular, the approach is not identified with the satisfaction of (partial) necessary conditions only, as are the so-called first-order-methods.

Our example problem was easily handled using ordinary (Newton-Raphson) numerical procedures. Also, in this case, the issue of local versus global extremum does not arise since the equations are sufficient as well as necessary. On the other hand, serious difficulties may be encountered in the numerical solution of structures optimization problems where either the behavior toward convergence is poor (common in constrained design problems), or where sufficiency conditions are not known (e.g., in the design of solid plates). The numerical treatment of problems in both of these categories is to be considered in a later paper.

## References

[1] Niordson, F. I. and Pedersen, P., "A Review of Optimal Structural Design," DCAMM Rept. 31, Sept. 1972, Technical Univ. of Denmark, Lyngby, Denmark.

[2] Haug, E. J., Jr., Pan, K. C., and Streeter, T. D., "A Computational Method for Optimal Structural Design: Piecewise Uniform Structures," *International Journal of Numerical Methods in Engineering*, Vol. 7, No. 2, Nov.-Dec. 1972, pp. 171–184.

[3] Maier, G., Zavelani-Rossi, A., and Benedetti, D., "A Finite Element Approach to Optimal Design of Plastic Structures in Plane Stress," *International Journal of Numerical Methods in Engineering*, Vol. 4, No. 4, July-Aug. 1972, pp. 455–473.

[4] Dafalias, Y. F. and Dupuis, G., "Minimum-Weight Design of Continuous Beams Under Displacement and Stress Constraints," *Journal of Optimization Theory and Applications*, Vol. 9, No. 2, Feb. 1972, pp. 137–154.

[5] Ashley, H. and McIntosh, S. C., Jr., "Applications of Aeroelastic Constraints in Structural Optimization," *Proceedings of the 12th International Congress of Applied Mechanics*, Springer-Verlag, Berlin, 1969, pp. 100–113.

[6] Rossow, M. P., "A Finite Element Approach to Optimal Structural Design," Ph.D. thesis, 1973, The Univ. of Michigan, Ann Arbor, Mich.

[7] Taylor, J. E., "Maximum Strength Elastic Structural Design," *Proceedings of the ASCE*, Vol. 95, No. EM3, June 1969, pp. 653–663.

[8] Prager, W. and Taylor, J. E., "Problems of Optimal Structural Design," *Journal of Applied Mechanics*, Vol. 35, No. 1, March 1958, pp. 102–106.

[9] Sheu, C. Y. and Prager, W., "Minimum-Weight Design with Piecewise Constant Specific Stiffness," *Journal of Optimization Theory and Applications*, Vol. 2, No. 3, May 1969, pp. 179–186.

[10] Mroz, Z., "Multi-parameter Optimal Design of Plates and Shells," *Journal of Structural Mechanics*, Vol. 1, No. 3, 1972, pp. 371–392.

[11] Irons, B. M., "Engineering Application of Numerical Integration in Stiffness Method," *AIAA Journal*, Vol. 4, No. 11, Nov. 1966, pp. 2035–2037.
[12] Mansfield, E. H., "Optimum Variable Thickness Reinforcement Around a Circular Hole in a Flat Sheet Under Radial Tension," *Quarterly Journal of Mechanics and Applied Mathematics*, Vol. 24, Pt. 4, 1971, pp. 499–507.

# Coherence Measurements in an Axisymmetric Wake

J. B. ROBERTS*
*University of Sussex, Falmer, Brighton, Sussex, England*

## 1. Introduction

STUDIES of the structure of the wake behind axisymmetric blunt-based bodies extend over a period of many years. Much of the early work concentrated on low Reynolds number flow (e.g., see Ref. 1) and was mainly confined to flow visualization studies. A notable exception is the work of Winny[2] who examined concurrent signals from two hot wires in an attempt to detect the wake structure behind a sphere, at high Reynolds numbers.

More recently a number of experimental studies of axisymmetric wake flows at high Reynolds numbers have been published[3–9] and various aerospace problems which have arisen in the last few years have stimulated renewed interest in this aspect of bluff-body aerodynamics.[9]

Previous studies have established, by spectral analysis of single hot wire signals, that a definite periodicity exists in axisymmetric wake flows behind blunt-based bodies but the actual wake structure, for Reynolds numbers above a few hundred, is still unknown. It has been suggested by Calvert[7] and others[5] that the analysis of concurrent signals from two hot wires, and in particular the cross-spectral analysis of such signals, is likely to yield considerable information on the wake structure. The purpose of this Note is to report the results of a series of such measurements. This approach is, of course, in the spirit of Winny's early work but advantage can now be taken of developments which have occurred in hot wire instrumentation and in the statistical analysis of random signals. Winny's work was restricted to a visual examination of concurrent hot wire signals and this enabled only very rough estimates of phase relationships to be made. In contrast, in the present work, the very powerful techniques of digital spectral and cross-spectral analysis are employed to yield precise quantitative information on the frequency dependence of the correlation and phase relationships between hot wire signals.

## 2. Experimental Equipment

The experimental measurements were performed in a closed circuit wind tunnel having a test section measuring 3 ft square by 14.5 ft long. The background turbulence intensity was less than 0.5% throughout the test section.

A 3-in.-diam stainless steel disk, with a sharp edged upstream face, was mounted on wires, normal to the flow, at a position 6 ft downstream of the inlet to the test section, and in the center of the tunnel. By observing the reflection of a pair of crossed wires in the highly polished upstream face of the disk, with a telescope, this face was accurately aligned to be normal to the centerline of the tunnel test section.

Received March 27, 1973; revision received June 15, 1973.
Index category: Jets, Wakes, and Viscid-Inviscid Flow Interactions.
* Lecturer in Mechanical Engineering, School of Applied Sciences.

Near the station where measurements were to be taken a $\frac{1}{2}$-in. diam rod was fixed across the tunnel to support two hot wire probes. The hot wire systems used were commercial Disa constant temperature anemometer 55AO1 sets and the probes used were standard Disa miniature hot wires with active elements of 0.5-$\mu$m-diam platinum plated tungsten wire, 1.25 mm long.

The wind-tunnel speed was monitored by a Betz manometer, which indicated the difference between static pressures in the test section and the settling chamber. This had previously been calibrated against a pitot-static probe in the test section.

## 3. Data Analysis

Let $u(t)$ denote the variation of the longitudinal velocity component with time recorded by one hot wire probe. Assuming $u(t)$ is a realization of a stationary random process, with mean $m$, the power spectrum of $u(t)$ is defined as

$$S(f) = 2\int_{-\infty}^{\infty} w(\tau)\cos(2\pi f\tau)\,d\tau$$

where $w(\tau)$, the covariance function of $u(t)$ is given by

$$w(\tau) = E\{[u(t)-m][u(t+\tau)-m]\}\dagger$$

For two hot wire signals, $u_1(t)$ and $u_2(t)$, with means $m_1$ and $m_2$, and power spectra $S_1(f)$ and $S_2(f)$, respectively, the cross-spectrum is defined as

$$S_{12}(f) = 2\int_{-\infty}^{\infty} w_{12}(\tau)\exp(-i2\pi f\tau)\,d\tau$$

where

$$w_{12}(\tau) = E\{[u_1(t)-m_1][u_2(t)-m_2]\}$$

The nondimensional coherence function, $C$, is defined as

$$C = S_{12}(f)/[S_1(f)S_2(f)]^{1/2} = C_r + iC_i$$

Power spectra and cross-spectra of the hot wire signals, together with the related coherence function, were obtained from the spectral analysis system described by Roberts and Surry.[10] The data was analyzed in real time, using analog lines to a remote analog-to-digital converter and computer. Tests proved that the analog lines introduced negligible degradation of data, over the frequency range considered here.[10]

The conventional Blackman and Tukey correlation technique was used to generate the power and cross-spectral estimates, correlation computations being performed between successive samples.

## 4. Discussion of Results

Throughout the experiments the tunnel mean wind speed $U$ was maintained at 50 fps, giving a Reynolds number based on disk diameter of $7.8 \times 10^4$. A variety of mean flow and intensity traverses were made downstream of the disk to check the symmetry of the wake.

### a. Single probe results

Initially, the periodicity in the wake was investigated by performing a power spectrum analysis on the signal from a single hot wire probe, at various positions in the wake. In view of the uncertainties in hot wire measurements in high intensity turbulence, measurements were confined to probe positions at least nine diameters downstream of the disk ($X/D = 9$); here the turbulence intensity was everywhere less than 10%.

A definite peak was observed in the power spectrum of the probe signal, at all probe positions in the wake except those directly on the disk axis of symmetry. The frequency $f$ of this peak was independent of probe position, with a Strouhal number $S = fD/U$ of 0.135, in agreement with the observations of Calvert.[7] On traversing the probe radially outwards, at a fixed $X/D$, the height of the spectral peak was found to increase

† $E\{\ \}$ denotes the expectation, or ensemble averaging, operator.